

Design of 10×10 Massive MIMO Array in Sub-6 GHz Smart Phone for 5G Applications

Tamer Gaber Abouelnaga^{1, 2, *}, Ibrahim Zewail², and Mona Shokair³

Abstract—In this paper, a design of a dual-band 10×10 antenna array for 5G Massive Multi-Input Multi-Output (MIMO) applications in the mobile phone is presented. The designed array is proposed to cover the sub-6 GHz bands (LTE bands 42/43 and LTE band 46). To realize MIMO operation in these three LTE bands, ten ring loop antenna elements are integrated into a limited space cell phone circuit board. Due to the implementation of spatial diversity techniques on the antenna elements, better isolation can be achieved. The proposed array was simulated, fabricated, and measured. It achieved good MIMO performances, such as ergodic channel capacities higher than 27.1 bps/Hz and 57.6 bps/Hz for LTE bands 42/43 and LTE band 46, respectively. Also, the achieved Envelope Correlation Coefficient (ECC) is lower than 0.006. Moreover, it exhibited good isolation below -26 dB. The effects of the user's hand phantom on the proposed array performance are also studied in two scenarios: Single Hand Mode (SHM) and Dual Hands Mode (DHM). The simulated results indicate that the proposed MIMO array can still achieve good MIMO performances in the presence of DHM and SHM. The Specific Absorption Rate (SAR) is also presented.

1. INTRODUCTION

Recently, the incoming generation of 5G communication networks has a new vision that lies in providing extremely high data rates about GHz order, higher capacity, lower latency, hundred percent coverage, and sufficient increase in the user's Quality of Service (QoS) compared with the 4G LTE networks [1–3]. Moreover, smartphones today have a large variety of applications such as navigation, communication services, entertainment, and mobile financial services. Therefore, smartphones should have the ability to improve signal transmission performances and achieve multiband operation. This issue is now the hotspot of research in the field of wireless communications. Further, the channel capacity and spectrum efficiency can be effectively increased by using massive MIMO techniques [4–7].

Some designs of MIMO antenna array have been proposed for 5G smartphones. Among different applicable solutions, massive MIMO arrays are particularly useful for this application, which are able to improve the channel capacity and spectrum efficiency. In fact, MIMO technique is a key technology for the future 5G networks, based on using a large number of antenna elements into the smartphone device and the base station. Actually, arranging these antennas in a limited space will lead to deteriorated efficiencies and isolation. The vital technical difficulty here is how to arrange antenna elements to achieve good performances. In 4G Long Term Evolution (LTE) networks, the conventional 2×2 MIMO arrays were used, but it cannot afford high data rates. Therefore, 6×6 MIMO, 8×8 MIMO, 10×10 MIMO, or 12×12 MIMO arrays are currently necessary [8, 9]. There are three commonly used bands, LTE 42 (3.4–3.6 GHz), LTE 43 (3.6–3.8 GHz), and LTE 46 (5.15–5.925 GHz) in 5G. LTE42 is considered

Received 3 January 2021, Accepted 23 February 2021, Scheduled 9 March 2021

* Corresponding author: Tamer Gaber Abouelnaga (tamer@eri.sci.eg).

¹ Microstrip Circuits Department, Electronics Research Institute (ERI), Elnozha, Cairo, Egypt. ² Higher Institute of Engineering and Technology, Kafr El-Shiekh, Egypt. ³ Faculty of Electronic Engineering, El-Menoufia University, Menouf 32952, Egypt.

a potential spectrum band for the 5G Massive MIMO so that it has been used with many design shapes of MIMO antenna arrays [4].

On the other hand, LTE 46 is also selected as a prospective band to support the 5G MIMO design. Recently, some designs of MIMO antenna array have been proposed for 5G smartphones. Table 1 shows the details of some related works about this topic. As shown in this table, the researchers have proposed different numbers of antenna elements (4 or 8 or 10 or 12 elements) to cover one 5G band as in [10, 11], or two 5G bands as in [4], or three 5G bands as in [12, 13]. Also, the dimensions of the smartphone as shown in Table 1 are varied, where the smallest size is $136 \times 68 \text{ mm}^2$, and the largest size is $150 \times 80 \text{ mm}^2$. The maximum isolation and smallest Envelope Correlation Coefficient (ECC) values were achieved in [14] which used 8 antenna elements to cover only LTE band 42.

Table 1. Previous smartphones 5G MIMO antenna array.

Reference	Number of Elements	Bandwidth (GHz)	Isolation (dB)	ECC	Ground Size (mm^2)
[4]	8	LTE 42/43, LTE 46	12 dB	< 0.1 (LB), < 0.04 (HB)	150×75
[10]	8	LTE 42	15 dB,	< 0.2	145×70
[14]	8	LTE 42	20 dB	< 0.0125	150×75
[11]	4	LTE 42	17 dB	< 0.1	150×73
[12]	12	LTE 42/43, LTE 46	12 dB	< 0.15 (LB), < 0.1 (HB)	150×80
[15]	8	LTE 42/43, LTE 46	10 dB	< 0.2 (LB), < 0.05 (HB)	150×76.6
[16]	10	LTE 42/43, LTE 46	11 dB	< 0.15 (low band), < 0.05 (high band)	150×80
[17]	10	LTE 42/43, LTE 46	11 dB	< 0.1	150×62.7
[13]	8	n77 (3.55–4.2 GHz)/ n78/n79 3.6–4.2 GHz, (4.4–4.9 GHz) and LTE 46	10 dB	< 0.1	136×68

In this paper, a 10-ports dual-band massive MIMO antenna array is proposed to cover both the LTE bands 42/43 and LTE 46 for 5G mobile handsets. Here, ten antenna elements are integrated into the PCB of the handset. One type of antenna is used, namely, ring loop antennas located at different locations. The proposed MIMO antenna array is simulated, fabricated, and measured. The simulated results are obtained by CST Microwave Studio. The S -parameters are measured and compared with the simulated counterpart. Vital results, such as ergodic channel capacities, are higher than 42.5 bps/Hz and 60 bps/Hz across the operation bands and achieve good MIMO performances through ECC lower than 0.006. Moreover, it exhibits good isolation below -26 dB. The effects of the user's hand phantom on the proposed array are also studied in two scenarios: Single Hand Mode (SHM) and Dual Hands Mode (DHM). The result indicates that the proposed MIMO array can still achieve good MIMO performances under the phantom effect.

2. PROPOSED ANTENNA ARRAY DESIGN

2.1. Array Structure

The complete architecture and physical dimensions of the suggested 10-antenna array are shown in Figure 1. The proposed architecture of the mobile phone has dimensions $150 \text{ mm} \times 80 \text{ mm} \times 8 \text{ mm}$, with

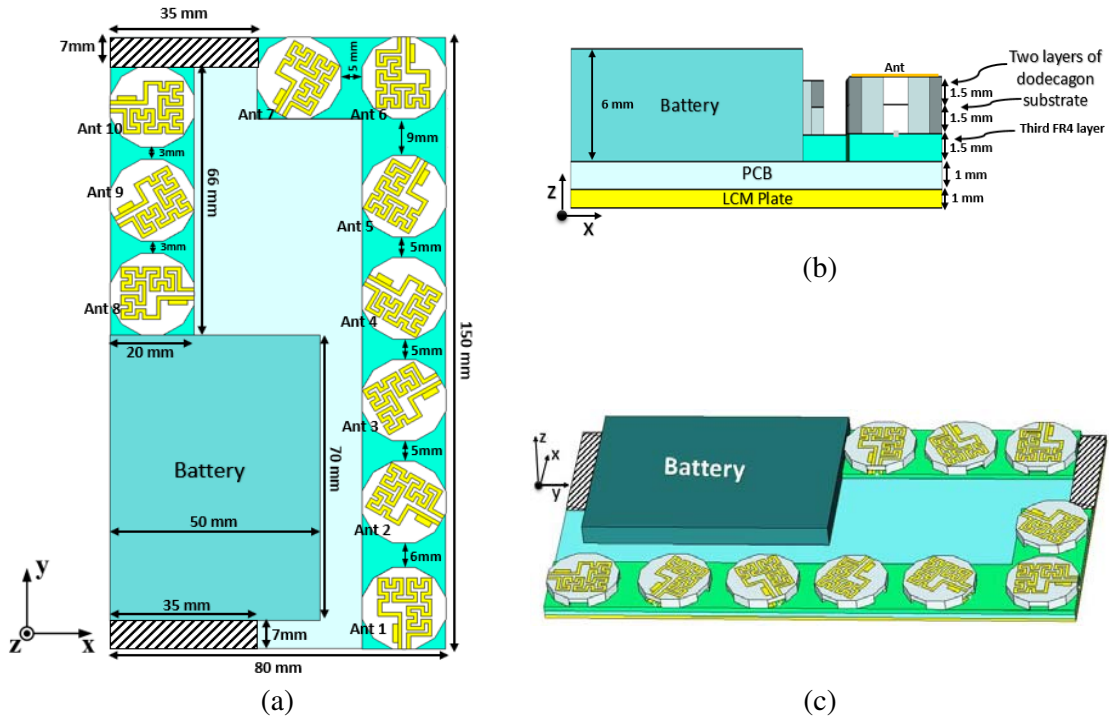


Figure 1. (a) Architecture and detailed dimensions of the proposed 10-antenna array, (b) side view, (c) geometry of the mobile phone.

a 5.7-inch display, which is a usual size for smartphones. The LCD screen and cell phone battery are considered as metal solid. The LCD screen is considered as metal solid as in [10, 18], where the LCD module is composed of two parts, namely, the LCD shield (which adheres to the ground plane and is made of stainless steel) and the LCD panel (which adheres to the LCD shield and is made of glass). In Figure 1(a), the two hatched blocks, each of size $7\text{ mm} \times 35\text{ mm}$, are reserved for accommodating 2G/3G/4G MIMO antennas, which will be considered as copper. The lower left block is reserved for a battery with dimensions $50 \times 70 \times 6\text{ mm}^3$. The battery block is defined as copper in the simulation.

2.2. Antenna Element

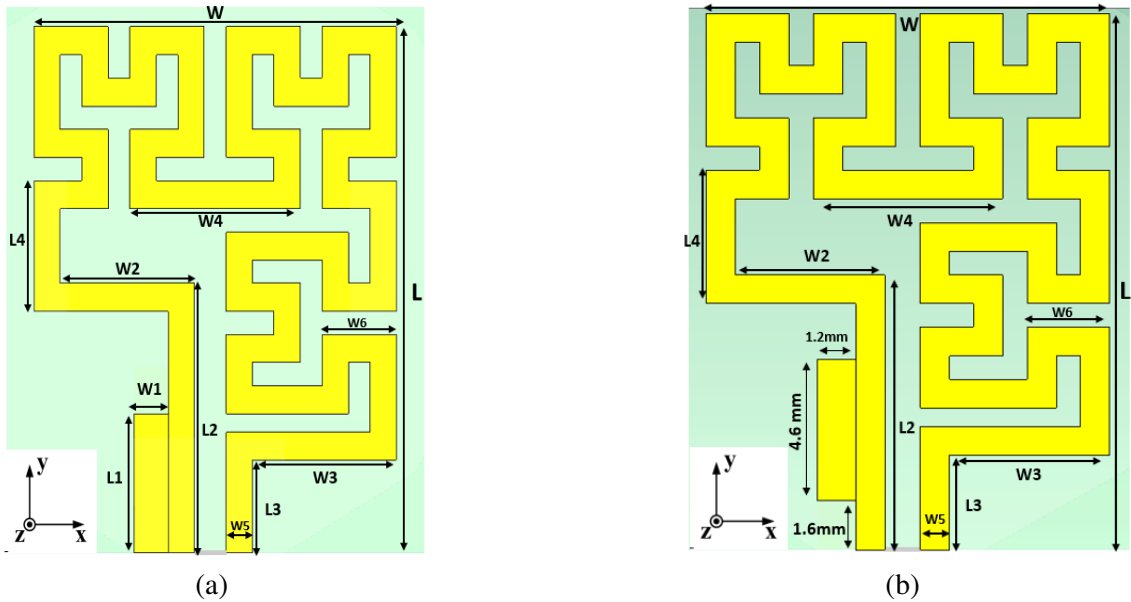
The detailed geometry of the proposed antenna is shown in Figure 2(a), and the dimensions of the antenna are indicated in Table 2. The proposed antenna geometry is formed as a ring loop antenna, where Loop antenna advantages and less affected by the environment (human body, metal, etc.) and do not require grounding [10]. The designed loop is inspired by the space-filling curve (Hilbert curves) [19], of order 3. This design is proposed to operate as a dual-band antenna to cover LTE band 42 (3.4–3.6 GHz), LTE band 43 (3.6–3.8 GHz), and LTE band 46 (5.15–5.925 GHz) for the 5G smartphone applications. The antenna element is constructed as a stacked antenna as shown in Figure 3, where it consists of a lower printed loop antenna fabricated from copper material shown in Figure 2(a) and an upper loop antenna with dimensions shown in Figure 2(b), and between them two layers of an FR4 dodecagon substrate, each of 1.5 mm thickness, are inserted.

Moreover, the lower layer of dodecagon substrate is formed as shown in Figure 3 by cutting some parts of the dodecagon substrate to connect the SMA connectors with the lower printed loop antenna, where the effect of forming the substrate is taken into account. Forming the substrate shifts the resonant frequency and bandwidth. Also, the dodecagon shape is carefully selected, and it has 12 sides which gives the ability to change the orientation of the antenna by 30° .

Figure 4 investigates the simulated S parameter of the designed antenna array, using the full-wave Computer Simulation Technology (CST) microwave studio version 2018. Figure 4(a) shows the S -parameters of the ten-antenna array, where the reflection coefficients of Ant. 1, Ant. 2, Ant. 3, Ant. 4,

Table 2. Dimensions of ring loop antenna.

Item	Value
L	17.4 mm
W	12.8 mm
$L1$	4.6 mm
$L2$	8.9 mm
$L3$	3.1 mm
$L4$	4.3 mm
$W1$	1.2 mm
$W2$	4.8 mm
$W3$	5.1 mm
$W4$	6 mm
$W5$	0.9 mm
$W6$	2.6 mm

**Figure 2.** Antenna geometry. (a) The lower loop antenna, (b) the upper loop antenna.

Ant. 5, Ant. 6, Ant. 7, Ant. 8, Ant. 9, and Ant. 10 are shown. The -6 dB bandwidth covers the LTE band 42/43 and band 46. Figure 4(b) shows the isolation between the ten adjacent antennas, where good isolations are obtained. Also, good spatial diversity is achieved. The isolation values vary between -22 dB and -43 dB for the LTE band 42/43, and the values vary between -22 dB and -50 dB for the LTE band 46. Figures 5(a) and (b) show the surface current density distributions of the proposed ring loop antenna at resonant frequencies of 3.6 GHz and 5.5 GHz, respectively.

The fabricated MIMO array which consists of four layers is shown in Figure 6. The first layer is the PCB layer fabricated from FR4 (relative permittivity 4.4 and loss tangent 0.02.) It is covered with a layer of copper from the bottom, but from the top, the copper occupies the battery and 2G/3G/4G regions only. The second layer is fabricated from FR4. 10 copper antenna elements are printed on the top of that layer, and the antenna elements are connected with ten SMA connectors for testing. The third layer is made of ten dodecagons connected with each other; the dodecagon shape is formed by

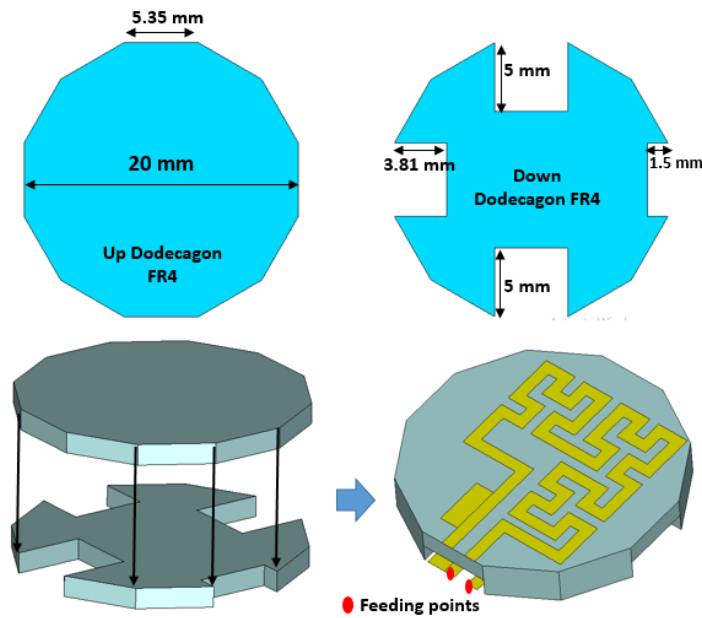


Figure 3. The printed stacked antenna and the formed dodecagon substrate.

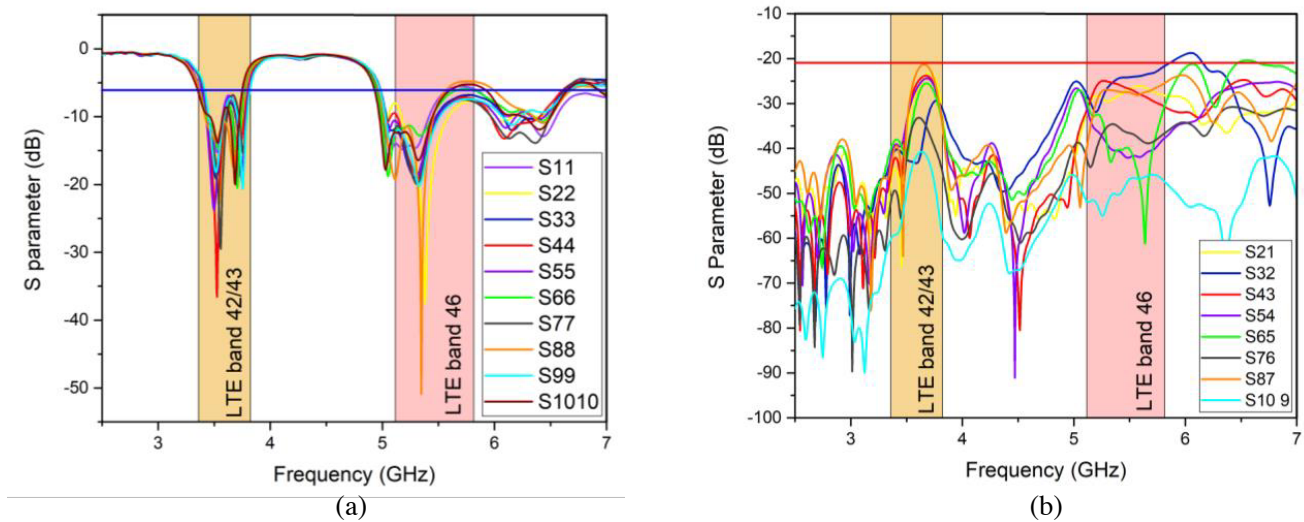


Figure 4. The simulated S parameter. (a) Reflection coefficient of the proposed ten-antenna array, (b) isolation between ports.

cutting some portions with a certain dimension. The fourth layer is ten loop antenna elements printed on a ten dodecagon FR4 substrate.

Figure 7 shows the integration steps of the proposed MIMO array design. Figure 7(a) shows the first step, where the second layer is put on the PCB layer; Figure 7(b) shows the instruction of the third layer over the second and first layers; then Figure 7(d) presents the complete structure of the 10 MIMO antenna array. Ten antenna elements are attached to each other and printed on the same surface of the same substrate layer. The array consists of three layers with the same size and same L-shape for easier alignment process as shown in Figures 6(b), (c), and (d). The first layer contains the ground plane at the bottom and the battery and 2G/3G/4G areas at the top as shown in Figure 6(a). Note that the ground plane presents the LCM plate of the phone.

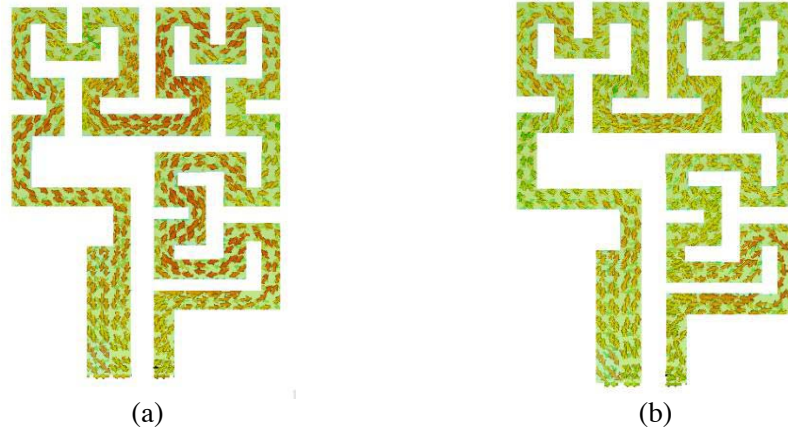


Figure 5. Surface current density distributions of the antenna at (a) 3.6 GHz, (b) 5.5 GHz.

3. RESULTS AND DISCUSSION

The proposed ten-antenna MIMO system is fabricated as shown in Figure 7 and tested. Due to the orientation of the antenna elements. The SMA connectors were added for measurement purposes only. However, in real mobiles, it will not be found. Also, the feeding structure is not considered in this paper. The measurements were done for only 6 antennas (for Ants 1, 2, 3, 6, 9, 10). In this section, the performance of the proposed dual-band MIMO antenna elements will be introduced by comparing the computed and measured results, where the measured S parameters (isolation and reflection coefficients) will be discussed, followed by evaluating the ECC of the ten-antenna elements, and the Ergodic Channel Capacities are also evaluated. Next, the radiation characteristics (total efficiency and radiation pattern) are investigated. Lastly, the effects of the user's hand on the proposed MIMO System are studied under two different modes: Single Hand Mode (SHM) and Double Hand Mode (DHM).

3.1. S Parameters

Figure 8 shows the measured S -parameters of the proposed prototype. In this figure, it is seen that the measured S -parameters agree well with the simulated counterpart. Even though some slight differences between the measured and simulated results are observed, they may be due to slight fabrication tolerance/inaccuracy and the insertion of the SMA connector. Figure 8(a) shows the measured and simulated reflection coefficients of the proposed dual-band MIMO antenna array. Table 3 introduces the -6 dB bandwidths for the measured and simulated antenna elements. The measured fraction bandwidths vary from 8.22% to 14.08% for the lower band and vary from 11.32% to 47.79% for the

Table 3. The measured and simulated -6 dB fraction bandwidth of the antenna elements.

Ant. No	LTE Bands 42/43						LTE Band 46					
	Measured (GHz)			Simulated (GHz)			Measured (GHz)			Simulated (GHz)		
	Band	f_o	%	Band	f_o	%	Band	f_o	%	Band	f_o	%
Ant 1	3.3–3.7	3.5	11.43	3.38–3.78	3.58	11.17	4.8–6.8	5.8	34.48	4.95–5.58	5.265	11.97
Ant 2	3.4–3.8	3.6	11.11	3.4–3.8	3.6	11.11	4.9–5.6	5.25	13.33	4.94–6.68	5.81	29.95
Ant 3	3.3–3.8	3.55	14.08	3.4–3.81	3.61	11.37	4.7–6.9	5.8	37.93	4.98–6.64	5.81	28.57
Ant 6	3.4–3.9	3.65	13.70	3.37–3.77	3.57	11.20	4.3–7	5.65	47.79	4.94–5.8	5.37	16.01
Ant 9	3.5–3.8	3.65	8.22	3.41–3.82	3.62	11.34	4.9–5.9	5.4	18.52	4.98–6.7	5.84	29.45
Ant 10	3.5–3.8	3.65	8.22	3.35–3.75	3.55	11.27	5–5.6	5.3	11.32	4.93–5.7	5.315	14.49

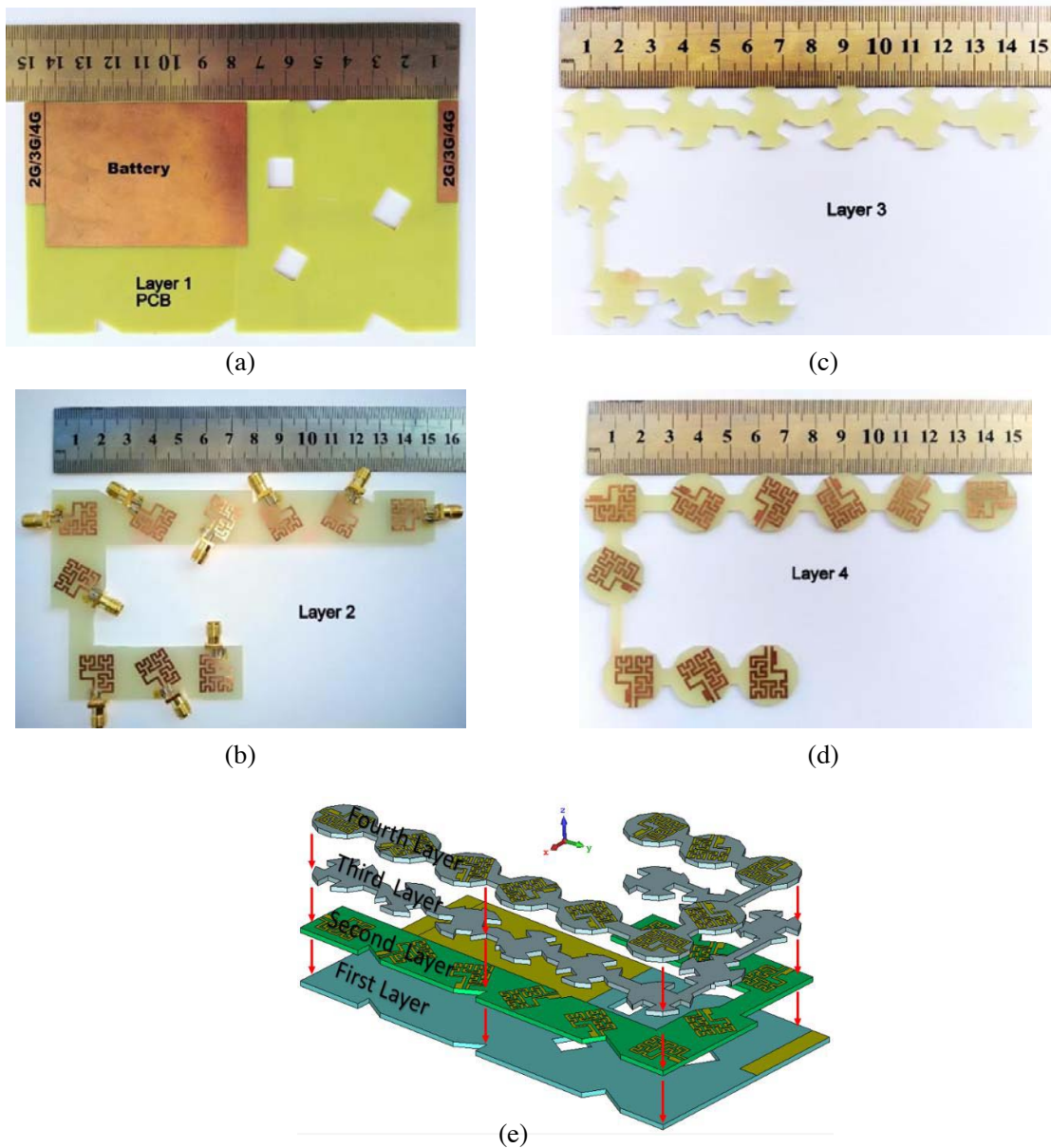


Figure 6. MIMO antenna layers. (a) PCB (layer 1), (b) lower loop antenna with SMA connectors (layer 2), (c) formed dodecagon FR4 substrate (layer 3), (d) upper loop antenna printed on dodecagon FR4 substrate layer (layer 4), (e) the integration of MIMO antenna array layers.

higher band, which cover the LTE bands 42/43 and LTE band 46. On the other hand, the simulated fraction bandwidths vary from 11.11% to 11.37% for the lower band and from 11.97% to 29.95% for the higher band.

The bandwidth variation over different antennas in LTE band 46 seems too large, where the antenna element is a dual-band antenna and covers two frequency bands, the lower band (LTE 42/43) and higher band (LTE 46). The bandwidth is small at the lower band and large at the higher band. The antenna has a different orientation and may be affected by the surrounding areas and the separation between the array elements.

Figure 8(b) shows the corresponding isolations between the adjacent antennas of the dual-band antenna elements at LTE 42/43 and LTE 46 bands. As shown in this figure, the isolation was below -26 dB. Generally speaking, the measurement results show that the proposed MIMO design has good

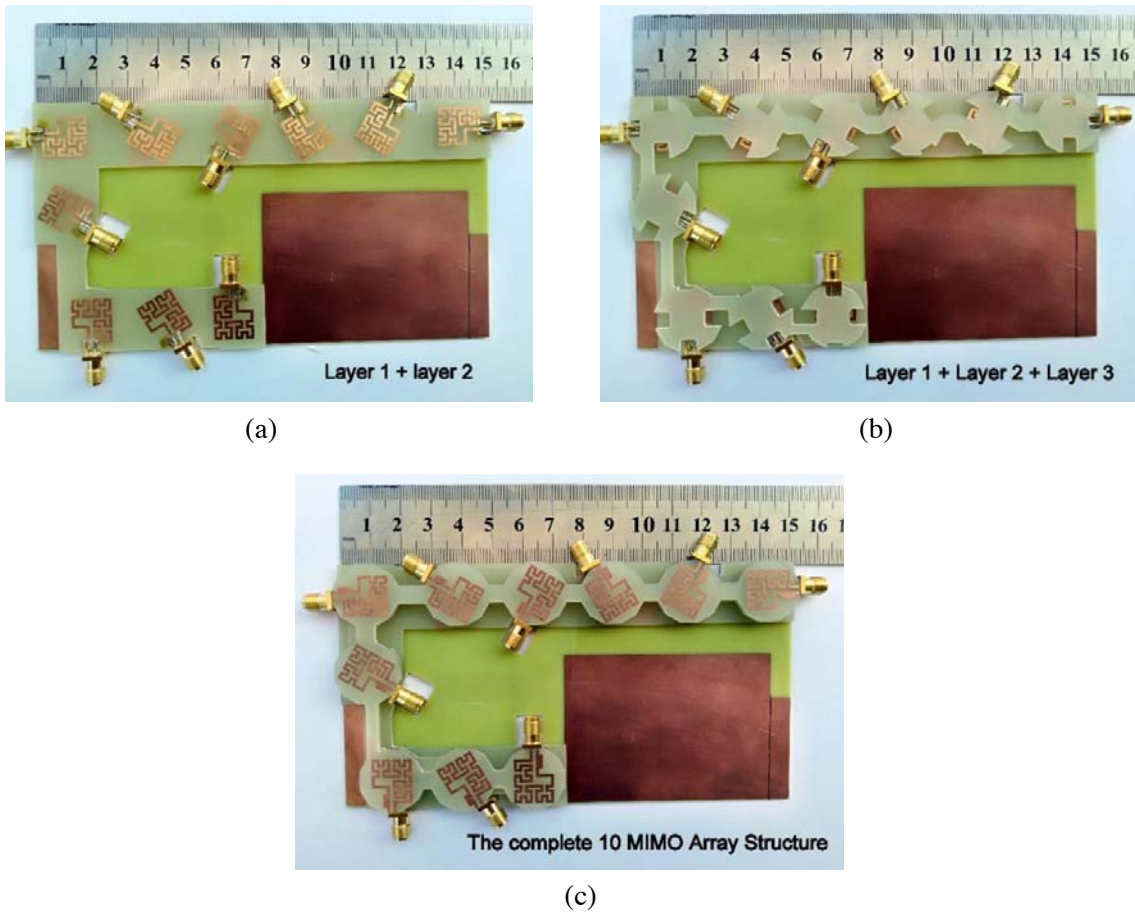


Figure 7. Integration steps. (a) Insertion of the second layer on the PCB layer, (b) insertion of the third layer over the second and first layers, (c) complete structure of the 10 MIMO array.

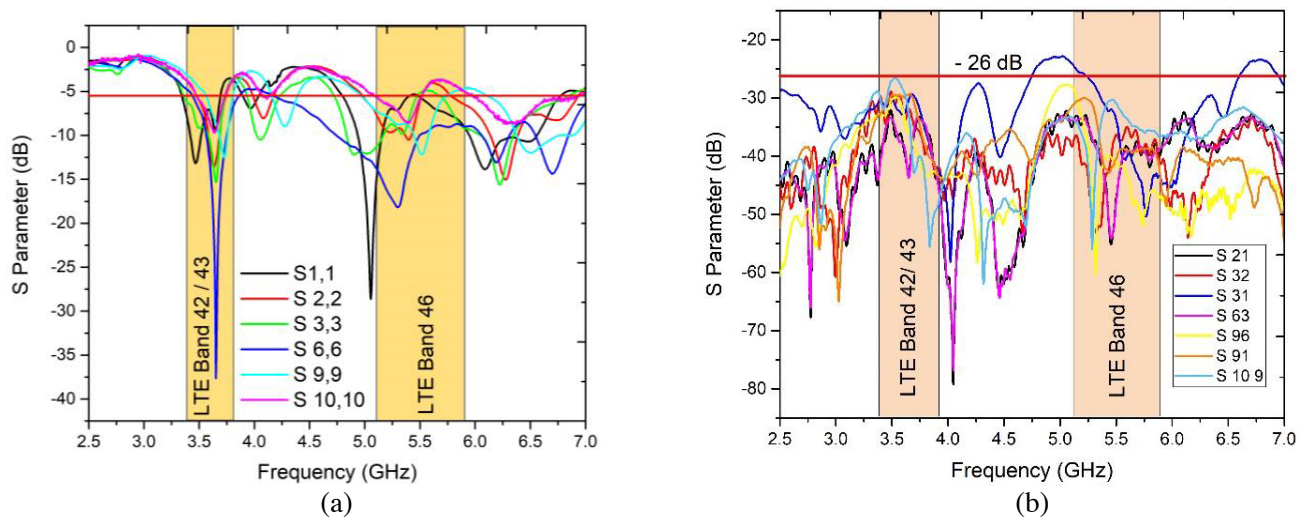


Figure 8. Measured S parameters of the dual-band. (a) Reflection coefficients, (b) isolation coefficients.

isolation and reflection coefficient performances that can fully cover the LTE bands 42/43 and LTE band 46.

3.2. Radiation Performances

Figure 9 shows the simulated total efficiencies of the 10×10 MIMO array for the ten antenna elements. The obtained results were done under the situation that only one antenna element is excited while the remaining nine antennas are matched. As shown in this figure, the total efficiencies vary approximately between 5% and 40% for the lower band (LTE bands 42/43). Further, the total efficiencies for the higher band (LTE band 46) vary approximately between 20% and 65%. Noting that the mutual coupling losses, mismatching, and radiation have affected the total efficiency evaluation. These results are compared with References [4, 11, 12, 14 15, 17]. Close results are obtained.

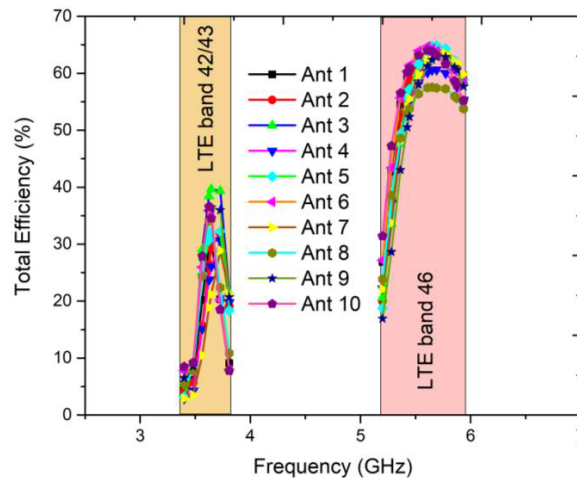


Figure 9. Total efficiencies of the dual-band 5G MIMO antennas.

The simulated phi-polarized and theta-polarized radiation patterns in the x - y plane of the proposed 10×10 MIMO design at two resonant frequencies 3.5 GHz for representing LTE 42/43 band and 5.3 GHz for representing LTE 46 band are illustrated in Figure 10 and Figure 11, respectively. Also, the directions of phi and theta radiation patterns in the x - y plane are illustrated in Figure 14. Noting that only the results of ants 1, 2, 3, 6, 9, and 10 are given. The antenna element's main beams at 3.5 GHz and 5.3 GHz are given in Table 4, thus good radiation diversity is achieved. The proposed ring loop antenna has demonstrated complementary and distinguishing patterns with good radiation features in the x - y plane.

In terms of the polarization characteristic, Figure 12 and Figure 13 show the co-polarization (C-pol) and cross-polarization (X-pol) patterns of the proposed array at two resonant frequencies 3.5 GHz and 5.3 GHz, respectively. The antenna elements have a good cross polarization level and dual-polarization purity at 3.5 GHz. At 5.3 GHz, even though the cross-polarization component rises, the polarization diversity is still effective for enhancing the isolation between the orthogonally polarized antennas.

3.3. MIMO Performances

Envelope Correlation Coefficient (ECC) has become a standard parameter for MIMO antennas. It is a measure of how correlated two different antennas' radiation patterns are. It measures the ECC for each two adjacent and non-adjacent antenna pairs. In this section, the MIMO performances such as ergodic channel capacity and ECCs for the proposed ten-element MIMO array are investigated and discussed to validate and evaluate the diversity performances. Here, the ergodic channel capacity is studied under a certain propagation scenario to demonstrate the data transmitting rate potential of the proposed MIMO array system. The formula in [20] was used to calculate the ergodic channel capacity, assuming that all the antenna elements have the same transmit power, and the Channel State Information (CSI)

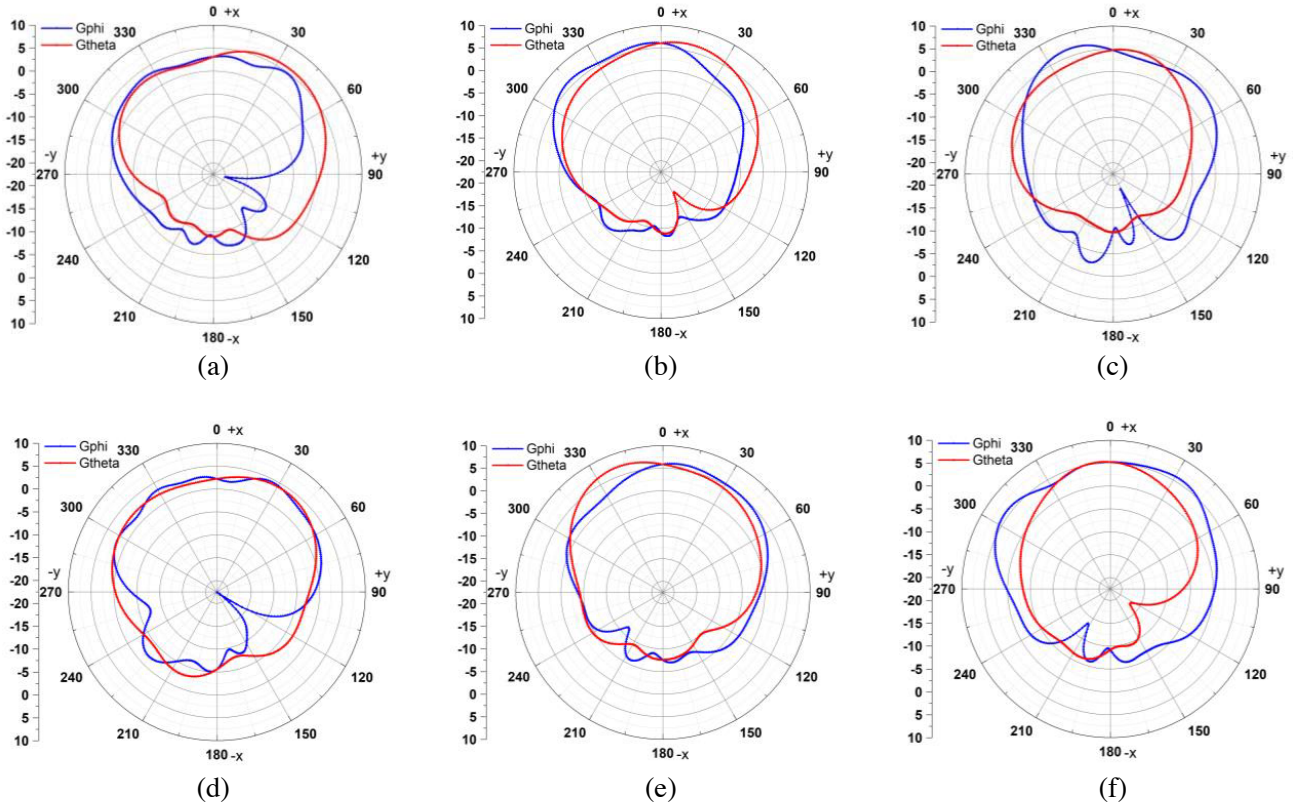


Figure 10. Simulated radiation patterns of the proposed 10×10 MIMO array at 3.5 GHz: (a) Ant 1, (b) Ant 2, (c) Ant 3, (d) Ant 6, (e) Ant 9, (f) Ant 10.

Table 4. Main beam angles of the proposed MIMO array.

Ant. No	3.5 GHz	5.3 GHz
Ant 1	$\text{phi} = 40^\circ$	$\text{phi} = 345^\circ$
Ant 2	$\text{phi} = 0^\circ$	$\text{phi} = 70^\circ$
Ant 3	$\text{phi} = 340^\circ$	$\text{phi} = 0^\circ$
Ant 6	$\text{phi} = 30^\circ$	$\text{phi} = 30^\circ$
Ant 9	$\text{phi} = 10^\circ$	$\text{phi} = 345^\circ$
Ant 10	$\text{phi} = 30^\circ$	$\text{phi} = 300^\circ$

is unknown for the transmitter. Rayleigh fading environment [21] is assumed for independently and Identically Distributed (IID) channels. The entries of Rayleigh fading channel are circularly symmetric complex Gaussian random variables with zero mean and variance of $1/2$ per dimension. The channel capacity is calculated at different values of Signal to Noise Ratio (SNR) equal to 20, 23, 26 dB. The channel capacities are obtained by averaging 100000 (IID) Rayleigh fading realizations for 10×10 MIMO antenna array in the desired bands (LTE band 42/43 and LTE band 46). Figure 15 and Table 5 show the calculated ergodic channel capacities for the ten antenna elements with different SNR values. It is observed that the proposed MIMO array (10×10) achieves peak capacities of 27.1 bps/Hz and 57.6 bps/Hz with SNR = 20 dB for the LTE band 42/43 and LTE band 46, respectively. Table 5 shows that increasing the SNR from 20 dB to 23 dB, the peak channel capacity increases by 10.85% at LTE band 42/43. Also increasing the SNR by 3 dB from 23 to 26 dB, the peak channel capacity increases by

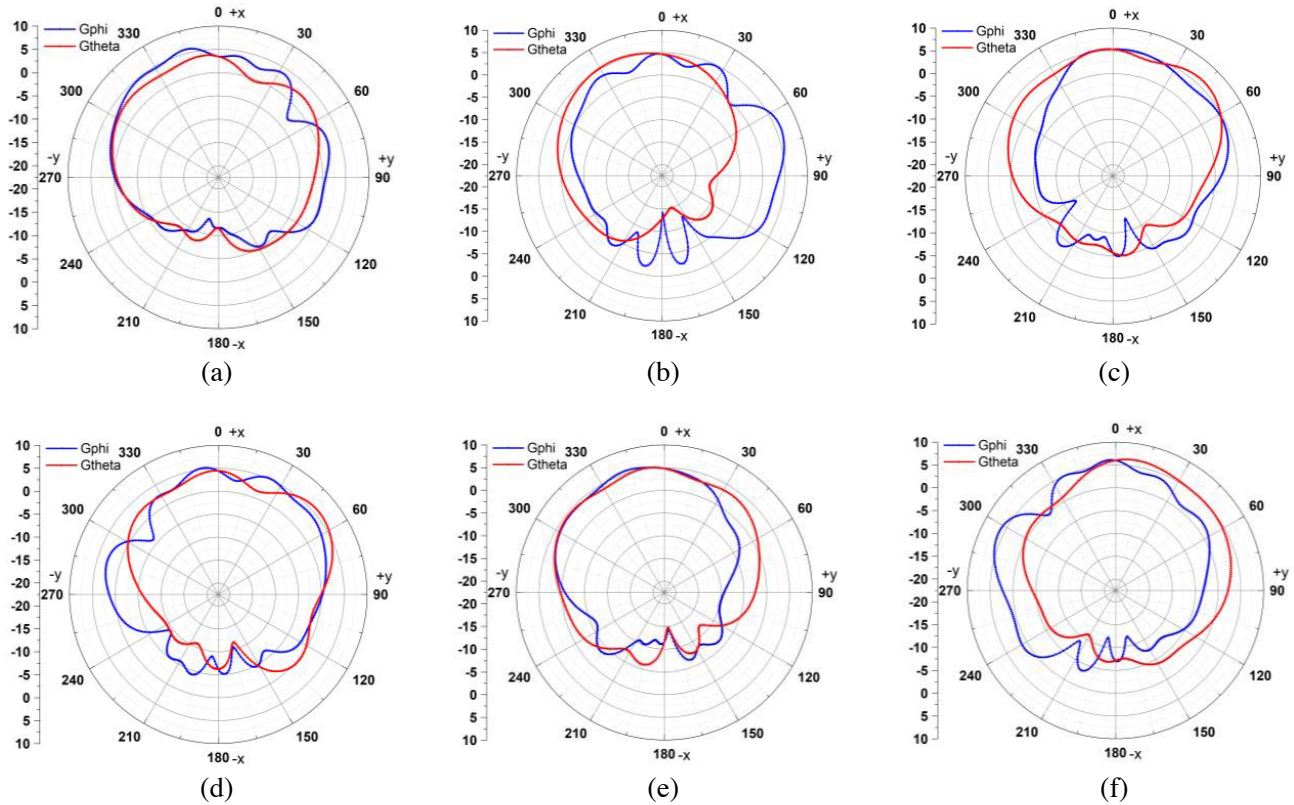


Figure 11. Simulated radiation patterns of the proposed 10×10 MIMO array at 5.3 GHz: (a) Ant 1, (b) Ant 2, (c) Ant 3, (d) Ant 6, (e) Ant 9, (f) Ant 10.

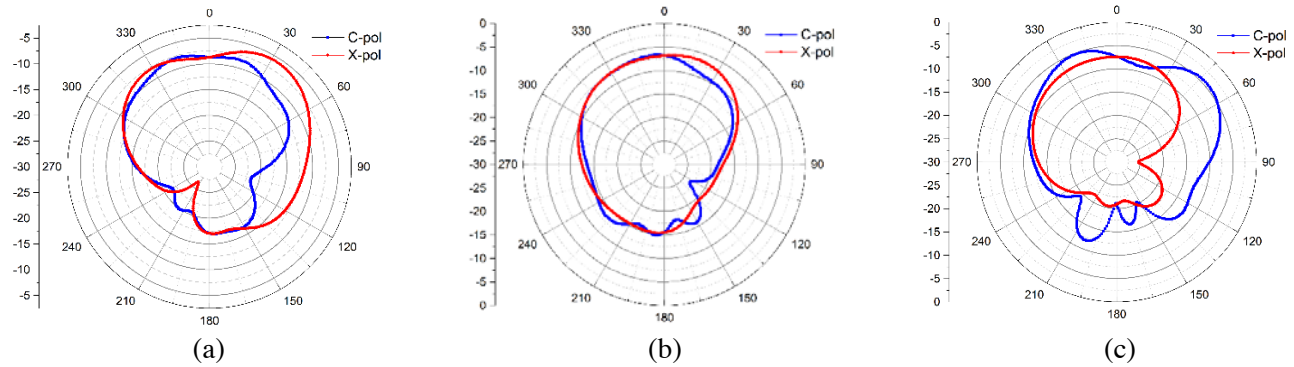


Figure 12. Simulated co-polarization (C-pol) and cross-polarization (X-pol) and cross-polarization patterns of the proposed 10×10 MIMO array at 3.5 GHz: (a) Ant 1, (b) Ant 2, (c) Ant 3.

10.1%. On the other hand, increasing the SNR from 20 dB to 23 dB, the peak channel capacity increases by 4% at LTE band 46. Also increasing the SNR from 23 to 26 dB, the peak channel capacity increases by 8.5%.

It is observed that the data throughput in the higher band (LTE 46) is greater than the lower band (LTE 42/43) because the absolute bandwidth of LTE bands 42/43 (400 MHz) is about two times lower than the absolute bandwidth of LTE band 46 (775 MHz). The proposed 10×10 MIMO design achieves much better multiplexing performances than traditional low-order MIMO.

On the other hand, the ECCs between the adjacent and non-adjacent antenna pairs are calculated for the two LTE bands (LTE band 42/43 and LTE band 46) as shown in Figure 16. The ECC can be

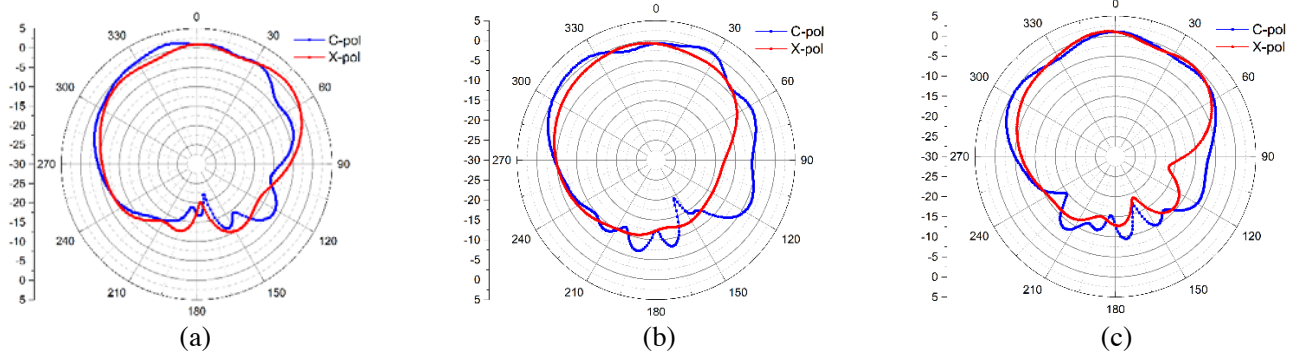


Figure 13. Simulated co-polarization (C-pol) and cross-polarization (X-pol) patterns of the proposed 10×10 MIMO array at 5.3 GHz: (a) Ant 1, (b) Ant 2, (c) Ant 3.

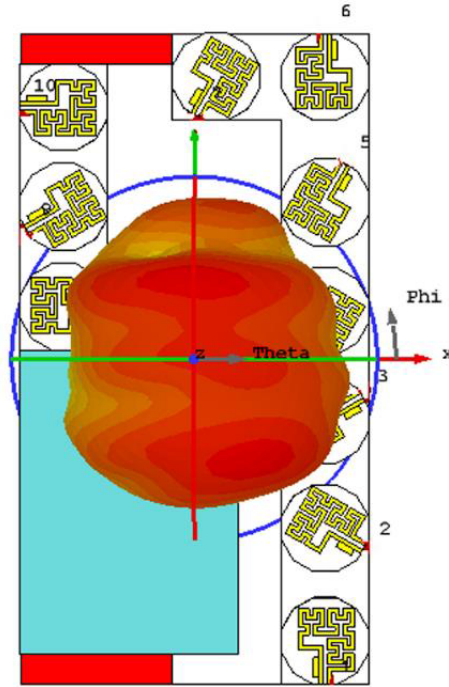


Figure 14. Phi-polarized and theta-polarized radiation pattern in the $x-y$ plane.

Table 5. Channel capacity peak values of the proposed 10×10 MIMO array with different SNR values.

Frequency Band	SNR = 20 dB	SNR = 23 dB	SNR = 26 dB
LTE 42/43	27.1 bps/Hz	30.4 bps/Hz	33.8 bps/Hz
LTE 46	57.6 bps/Hz	60 bps/Hz	65.6 bps/Hz

calculated from S -parameters and radiation efficiencies of MIMO antennas as follows [22]:

$$\rho_{eij} = \frac{|S_{ii}S_{yy}^* + S_jS_j^*|}{\sqrt{(1 - |S_{ii}|^2 - |S_{ji}|^2)(1 - |S_j|^2 - |S_{ij}|^2)} \eta_{radi} \eta_{radj}} \quad (1)$$

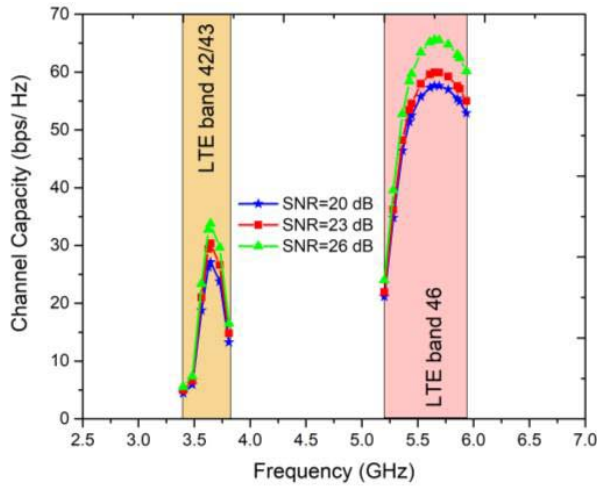


Figure 15. Channel capacity of the proposed 10×10 MIMO array.

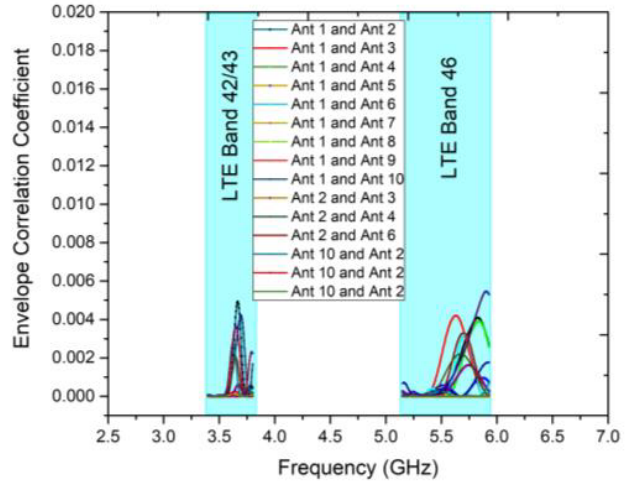


Figure 16. EEC of the proposed dual band 10×10 MIMO array.

In Figure 16, it is seen that the calculated ECC values are lower than 0.005 in the LTE bands 42/43 and lower than 0.006 in LTE band 46, which are acceptable criteria of ECC that should be lower than 0.5. From these results, the proposed 10×10 array can achieve desirable diversity characteristics.

3.4. User’s Hand Effects

In this section, the effects of the user’s hand on the antenna performances will be discussed. These effects are analyzed for the proposed MIMO array 5G data mode under two scenarios: Double Hand Mode (DHM) and Single Hand Mode (SHM) as shown in Figure 17.

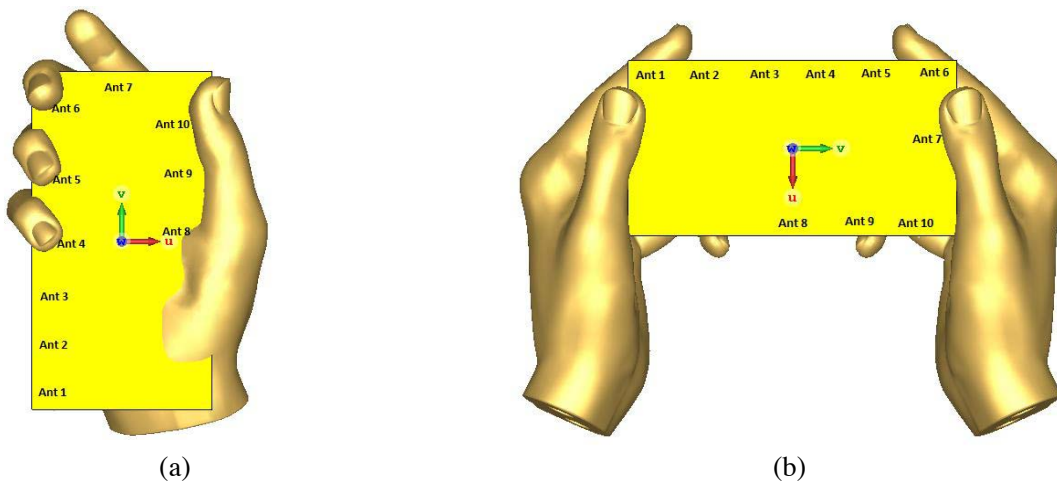


Figure 17. Two typical application scenarios under user’s hand operation. (a) Single hand mode (SHM), (b) double hand mode (DHM).

Firstly, we calculate the total efficiencies for the 10×10 MIMO array under the SHM and DHM in the LTE bands 42/43 and 46 as shown in Figure 18. As shown in Figure 18(a), using SHM scenario, Ant. 1 does not have direct contact with the hand phantom, so that it is not affected by the phantom, and it has a total efficiency better than 60% and shows good radiation performances.

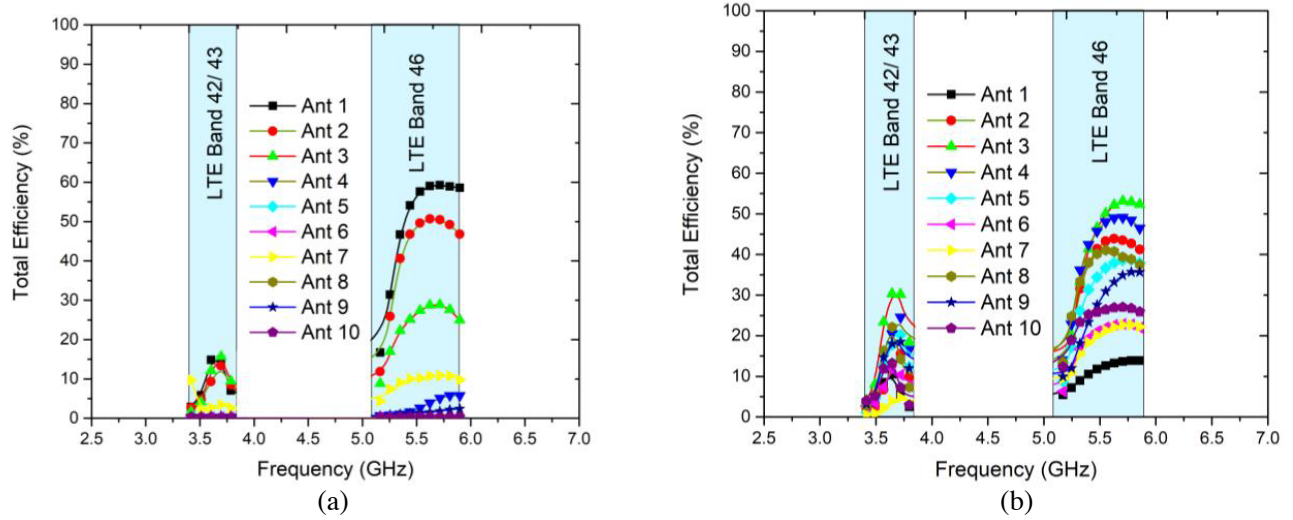


Figure 18. Total efficiencies of the proposed MIMO array with user's hand effect. (a) SHM, (b) DHM.

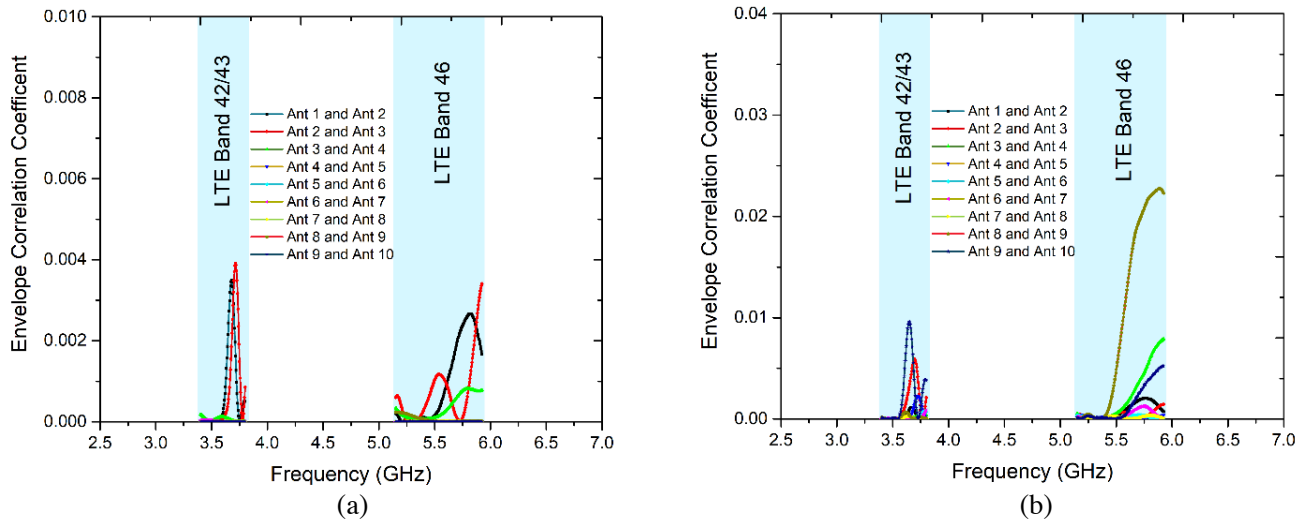


Figure 19. Simulated ECC under user's hand phantom effect. (a) SHM, (b) DHM.

Ant. 2 and Ant. 3 are also not close to the user's hand, and they have total efficiencies of more than 50% and 30%, respectively. Ants. 4, 5, 6, 7, 8, 9, 10 are in direct contact with the user's hand, so that their total efficiencies are below 20% in the LTE band 46, where they are deteriorated tremendously according to their proximity with the user's hand and the locations of the five fingers from each antenna. However, in the LTE band 42/43, all the antennas are affected by the user hand phantom, and their total efficiencies are below 20%. These results are because the hand's tissue is a very lossy medium and absorbs part of the power radiated by antenna elements, which affects the total efficiencies of the proposed 10×10 antenna array.

Furthermore, the DHM scenario is investigated in Figure 18(b). Ant. 1 is in direct contact with the user's hand so that its total efficiency is about 15%. Ants. 6, 7, 10 are also close to the hand phantom, and their total efficiencies have deteriorated to 30%. However, Ants. 2, 3, 4, 5, 8, 9 do not have direct contact with the hand phantom, thus yield good radiation performances with antenna efficiencies better than 36% and 20% through the LTE band 46 and LTE band 42/43, respectively. It is observed that the double hand phantom affect the total efficiencies of the proposed 10×10 MIMO antennas, and in

this case, it will operate as 6×6 arrays.

The simulated ECCs between the adjacent antennas of the proposed MIMO array under the effect of the user's hand phantom are investigated in Figure 19. Figure 19(a) shows the ECC results under the effect of SHM which are lower than 0.004 in the LTE bands 42/43 and LTE band 46. Also, Figure 19(b) indicates the ECC values for DHM condition which is lower than 0.0227 in the LTE bands 42/43 and LTE band 46. Thus, the ECCs results for the proposed MIMO design considering both SHM and DHM are acceptable criterion of ECC that should be lower than 0.5.

In Figure 20, the antenna gain patterns for the proposed array under SHM and DHM conditions are simulated at 3.5 and 5.3 GHz to demonstrate the spatial diversity characteristic under the effect of the user's hand. Figure 20(a) shows the antenna gain patterns for the SHM scenario, where Ants. 1, 2, and 3 radiate in different directions at 5.3 GHz, which mainly radiate in the $-y$, $-y$, and $-x$ directions, respectively, and achieve good spatial diversity. Further, Figure 20(b) shows the antenna gain patterns for DHM condition, Ants. 2, 3, 4, 5, 8, and 9 radiate in different directions and achieve good spatial

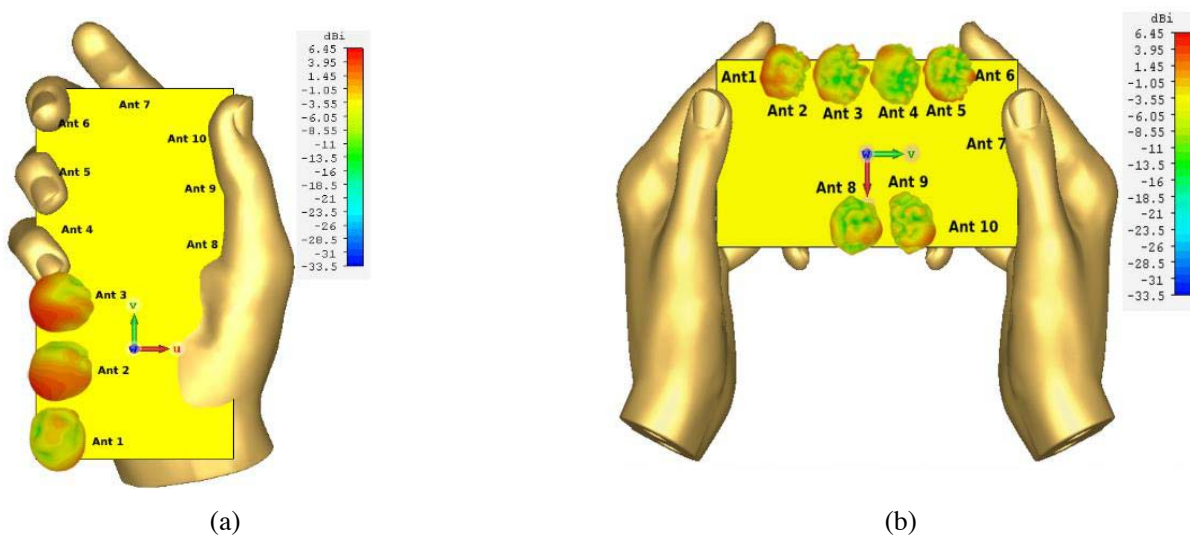


Figure 20. Simulated gain patterns of the proposed MIMO antenna array under (a) SHM, 5.35 GHz, (b) DHM, 5.35 GHz.

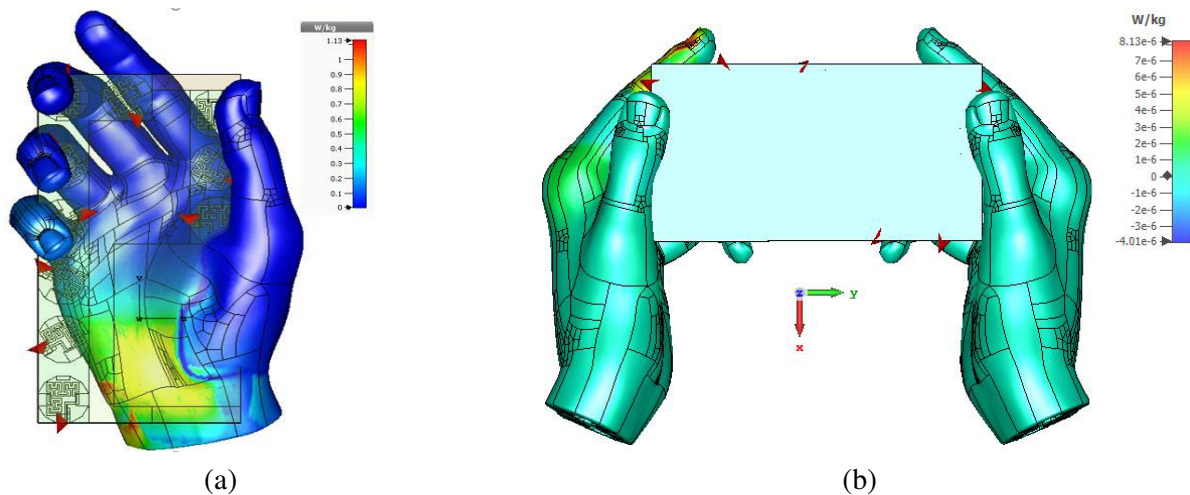


Figure 21. Simulated SAR at 3.5 GHz for ant 1 when averaged over 10 g of tissue under (a) SHM, (b) DHM.

diversity. These antennas mainly radiate in the $-y$, $-y$, $-x$, $+x$, $+y$, and between $+x$ and $+y$ directions at 5.3 GHz, respectively. Hence, it is demonstrated that the proposed MIMO array can operate as 6×6 MIMO under the DHM scenario. So, under the SHM and DHM scenarios, the proposed antenna elements achieve good pattern diversity characteristics.

Figure 21 shows the SAR levels that have been simulated for the handset (Ant. 1) where the antenna is close to the human hand. The simulation is performed with the presence of the human hand only, averaged over 10 g of tissue based on the IEC/IEEE 62704-1 averaging method [23], where the maximum permissible level is 1.6 W/kg averaged over the volume containing 1 g of tissue and 2.0 W/kg averaged over the volume containing 10 g of tissue. Figure 21 shows that the SAR value equals 1.125 W/kg and 0.0201 W/kg for the SHM scenario and DHM scenario, respectively, which is below the maximum standard values.

4. PERFORMANCE COMPARISON

Table 6 shows a comparison among the proposed 10×10 MIMO array and those previously reported. The proposed design has exhibited higher channel capacity in LTE band 46 as than all. Compared to Refs. [11, 14, 15], the proposed design has exhibited a higher efficiency in the LTE band 46. It has exhibited the lowest ECCs and isolation in the two bands LTE band 42/43 and LTE band 46 among all. Finally, the proposed 10×10 MIMO array covers the LTE band 46 for 5G applications.

Table 6. A comparison table between the proposed MIMO antenna and other references.

Reference	MIMO Order	Ground Size (mm ²)	-6 dB Bandwidth (GHz)		Total efficiency (%)		ECC		Maximum channel capacity (bps/Hz) at SNR = 20 dB	
					LTE 42/43	LTE 46	LTE 42/43	LTE 46	LTE 42/43	LTE 46
[4]	8×8	150×75	LTE 42	LTE 46	50–56	53–65	< 0.1	< 0.04	38.8	39.7
[14]	8×8	150×75	LTE 42	-	60	-	< 0.0125	-	34	-
[11]	4×4	150×73	LTE 42	-	58	-	< 0.1	-	16–19	-
[12]	8×8 (LB), 6×6 (HB)	150×80	LTE 42/43	LTE 46	41–82	47–79	< 0.15	< 0.1	37	29.5
[15]	8×8	150×76.6	41/42 (2.496–2.69), LTE 43		48–66, 44–59	-	< 0.2, < 0.05	-	38.3	-
[17]	8×10	150×62.7	LTE 42/43	LTE 46	52.4–71.7	48.9–75.4	< 0.1	< 0.1	43.3	41.6
[24]	16×16	150×75	LTE 42/43	-	30–53	-	< 0.3	-	72	-
Proposed	10×10	150×80	LTE 42/43	LTE 46	5–40	20–65	< 0.005	< 0.006	27.1	57.6

5. CONCLUSIONS

In this paper, a design of a dual-band 10×10 MIMO antenna array for 5G applications is presented to cover the sub-6 GHz bands (LTE bands 42/43 and LTE band 46). Due to the implementation of spatial diversity techniques on the antenna elements, better isolation has been achieved. The proposed array is simulated, fabricated, and measured. The measured results demonstrate good fraction bandwidth about 35% and 75% across the low band and high band, respectively. Vital results, such as ergodic channel capacities, are higher than 42.5 bps/Hz and 60 bps/Hz across the operating bands and achieve good MIMO performances through Envelope Correlation Coefficient (ECC). Moreover, it exhibits good isolation below -26 dB. The effects of the user's hand phantom on the proposed MIMO array are also studied in two scenarios: Single Hand Mode (SHM) and Dual Hands Mode (DHM). The results indicate that the proposed MIMO array keep good MIMO performances under the phantom effect.

REFERENCES

1. Al-Mejibli, I. and S. Al-Majeed, "Challenges of using MIMO channel technology in 5G wireless communication systems," *2018 Majan Int. Conf.*, 1–5, 2018, doi: 10.1109/mintc.2018.8472778.
2. Tang, W., S. Kang, J. Zhao, Y. Zhang, X. Zhang, and Z. Zhang, "Design of MIMO-PDMA in 5G mobile communication system," *IET Commun.*, Vol. 14, No. 1, 76–83, 2020, doi: 10.1049/iet-com.2018.5837.
3. Dadhich, A., M. Sharma, and J. K. Deegwal, "Design and investigation of wideband and multiband microstrip patch antenna for Bluetooth, TD-LTE, ITU and X-band applications," *Int. Conf. Emerg. Trends Eng. Innov. Technol. Manag. (ICET EITM-2017)*, Vol. 2, 409–412, ISBN 978-93-86724-30-4, 2017.
4. Zou, H., Y. Li, C. Sim, and G. Yang, "Design of 8×8 dual-band MIMO antenna array for 5G smartphone applications," *Int. J. RF Microw. Comput. Eng.*, Vol. 58, No. 1, 174–181, 2018, doi: 10.1002/mmce.21420.
5. Agiwal, M., A. Roy, and N. Saxena, "Next generation 5G wireless networks: A comprehensive survey," *IEEE Communications Surveys & Tutorials*, Vol. 18, No. 3, 1617–1655, 2016.
6. Singh, A. and C. E. Saavedra, "Wide-bandwidth inverted-F stub fed hybrid loop antenna for 5G sub-6 GHz massive MIMO enabled handsets," *IET Microwaves, Antennas Propag.*, Vol. 14, No. 7, 677–683, 2020, doi: 10.1049/iet-map.2019.0980.
7. Parchin, N. O., H. J. Basherlou, I. A. Yasir Al-Yasir, M. Sajedin, J. Rodriguez, and R. A. Abd-Alhameed, "Multi-mode smartphone antenna array for 5G massive MIMO applications," *14th Eur. Conf. Antennas Propagation, EuCAP 2020*, 4–7, 2020, doi: 10.23919/EuCAP48036.2020.9135754.
8. Al-Dulaimi, A., S. Al-Rubaye, Q. Ni, and E. Sousa, "5G communications race: Pursuit of more capacity triggers LTE in unlicensed band," *IEEE Vehicular Technology Magazine*, Vol. 10, No. 1, 43–51, 2015, doi: 10.1109/MVT.2014.2380631.
9. Serghiou, D., M. Khalily, V. Singh, A. Araghi, and R. Tafazolli, "Sub-6 GHz dual-band 8×8 MIMO antenna for 5G smartphones," *IEEE Antennas Wirel. Propag. Lett.*, Vol. 1225, 1–1, 2020, doi: 10.1109/lawp.2020.3008962.
10. Rao, L.-Y. and C.-J. Tsai, "8-loop antenna array in the 5 inches size smartphone for 5G communication the 3.4 GHz–3.6 GHz band MIMO operation," *2018 Progress In Electromagnetics Research Symposium (PIERS — Toyama)*, 1995–1999, Toyama, Japan, Aug. 1–4, 2018.
11. Ren, Z., A. Zhao, and S. Wu, "MIMO antenna with compact decoupled antenna pairs for 5G mobile terminals," *IEEE Antennas Wirel. Propag. Lett.*, Vol. 18, No. 7, 1367–1371, 2019, doi: 10.1109/LAWP.2019.2916738.
12. Li, Y., C. Y. D. Sim, Y. Luo, and G. Yang, "12-port 5G massive MIMO antenna array in sub-6 GHz mobile handset for LTE bands 42/43/46 applications," *IEEE Access*, Vol. 6, 344–354, 2017, doi: 10.1109/ACCESS.2017.2763161.
13. Sim, C. Y. D., H. Y. Liu, and C. J. Huang, "Wideband MIMO antenna array design for future mobile devices operating in the 5G NR frequency bands n77/n78/n79 and LTE band 46," *IEEE Antennas Wirel. Propag. Lett.*, Vol. 19, No. 1, 74–78, 2020, doi: 10.1109/LAWP.2019.2953334.
14. Zhao, A. and Z. Ren, "Size reduction of self-isolated MIMO antenna system for 5G mobile phone applications," *IEEE Antennas Wirel. Propag. Lett.*, Vol. 18, No. 1, 152–156, 2019, doi: 10.1109/LAWP.2018.2883428.
15. Li, Y., C. Y. D. Sim, Y. Luo, and G. Yang, "Metal-frame-integrated eight-element multiple-input multiple-output antenna array in the long term evolution bands 41/42/43 for fifth generation smartphones," *Int. J. RF Microw. Comput. Eng.*, Vol. 29, No. 1, 2019, doi: 10.1002/mmce.21495.
16. Li, Y., C. Y. D. Sim, Y. Luo, and G. Yang, "Multiband 10-antenna array for sub-6 GHz MIMO applications in 5-G smartphones," *IEEE Access*, Vol. 6, 28041–28053, 2018, doi: 10.1109/ACCESS.2018.2838337.
17. Li, Y. and G. Yang, "Dual-mode and triple-band 10-antenna handset array and its multiple-input multiple-output performance evaluation in 5G," *Int. J. RF Microw. Comput. Eng.*, Vol. 29, No. 2, 1–15, 2019, doi: 10.1002/mmce.21538.

18. Li, Y., C. Y. D. Sim, Y. Luo, and G. Yang, “High-isolation 3.5 GHz eight-antenna MIMO array using balanced open-slot antenna element for 5G smartphones,” *IEEE Trans. Antennas Propag.*, Vol. 67, No. 6, 3820–3830, 2019, doi: 10.1109/TAP.2019.2902751.
19. Alber, J. and R. Niedermeier, “On multidimensional curves with hilbert property,” *Theory Comput. Syst.*, Vol. 33, No. 4, 295–312, 2000, doi: 10.1007/s002240010003.
20. Sharawi, M. S., “Printed multi-band MIMO antenna systems and their performance metrics [wireless corner],” *IEEE Antennas Propag. Mag.*, Vol. 55, No. 5, 218–232, 2013, doi: 10.1109/MAP.2013.6735522.
21. Tian, R., B. K. Lau, and Z. Ying, “Multiplexing efficiency of MIMO antennas,” *IEEE Antennas Wirel. Propag. Lett.*, Vol. 10, 183–186, Sep. 2011, doi: 10.1109/LAWP.2011.2125773.
22. Chen, Q., et al., “Single ring slot-based antennas for metal-rimmed 4G/5G smartphones,” *IEEE Trans. Antennas Propag.*, Vol. 67, No. 3, 1476–1487, 2019, doi: 10.1109/TAP.2018.2883686.
23. IEC/IEEE International Standard, “Determining the peak spatial-average specific absorption rate (SAR) in the human body from wireless communications devices, 30 MHz to 6 GHz — Part 1: General requirements for using the finite-difference time-domain (FDTD) method for SAR calculations,” 2017.
24. Perhirin, S. and Y. Auffret, “8-antenna and 16-antenna arrays using the quad-antenna linear array as a building block for the 3.5-GHz LTE MIMO operation in the smartphone,” *Microwave and Optical Technology Letters*, Vol. 58, No. 1, 2562–2568, 2016, doi: 10.1002/mop.